A mesoscopic approach for the simulation of woven fibre composite forming

Philippe Boisse [a,*], Bassem Zouari [b], Alain Gasser [b]

[a] *Laboratoire de Mécanique des Contacts et des Solides, UMR CNRS 5514, INSA de Lyon Bâtiment Jacquard, Rue Jean Capelle, 69621 Villeurbanne Cedex, France*
[b] *Laboratoire de Mécanique de Systèmes et des Procédés, UMR CNRS 8106, ENSAM-ESEM, 8 rue Léonard de Vinci 45072 Orléans Cedex, France*

Abstract

A finite element simulation of composite woven reinforcement forming requires the knowledge of the fabric mechanical behaviour. In the presented mesoscopic approach, the tensile and shear mechanical behaviour of the elementary cell (mesoscopic level) are used in a finite element made of woven meshes. The principal stiffness of the fabric is the tensile rigidity. Because of the weaving, the tensile behaviour is non-linear. It is analysed by biaxial tensile tests and 3D finite element computations of the woven unit cells. The in plane shear rigidity of fabrics is very weak up to a limit angle. In this first stage, it is shown by optical measures that the yarns are subjected to rigid rotations. A second stage in which the yarns are laterally crushed leads to larger stiffness. A first simplified form of the dynamic equation is based only on tensile internal virtual work. A second one takes also shear internal work into account. A fabric square box forming simulation is performed with both approaches. It shows the importance to account for shear when the limit shear angle is exceeded.
© 2004 Elsevier Ltd. All rights reserved.

Keywords: A. Fabrics/textiles; A. Textile composites; C. Deformation; C. Finite element analysis (FEA); E. Resin transfer moulding; Forming simulations

1. Introduction

A lot of composites consist of woven reinforcements. As opposed to unidirectional reinforcements, these fibre fabrics permit to manufacture double curved parts accounting for the cohesion given by the weaving. The forming of theses composites makes use of the relative motion of the fibres that are possible in the case of a lack of matrix cohesion. The matrix can be absent (forming of dry fabric in the case of the R.T.M. process), not yet polymerized (prepreg draping) or made fluid by heating (thermoplastic matrix). In this paper, we consider the forming of dry fibre fabrics such as those used

for R.T.M. process. Nevertheless, most of the given results can be extended to non-polymerized prepreg forming and thermoplastic forming when the resin is fluid.

A simulation code permits to know the feasibility of a fabric forming without using trial and error method that is very expensive. It also gives information on the fibre directions after forming. These directions determine the final composite structure mechanical properties. In addition, the angles between warp and weft yarns influence the reinforcement permeability and consequently the mould filling. This delicate stage is well studied and several specific codes have been developed [1,2]. For the simulation of fabric forming, many codes use geometrical approaches (fishnet algorithms) [3–5]. These methods are fast and efficient. They permit to compute the angle between warp and weft yarns in order to compare this value to a limit angle over which the forming is

---

* Corresponding author. Tel.: +33 4 72 43 63 96.
E-mail address: philippe.boisse@insa-lyon.fr (P. Boisse).

no more possible without wrinkles. On the other hand, these methods do not take into account the material mechanical behaviour and the load boundary conditions. The aim of the present work is to present a mechanical approach that takes these two points into account. It is a mesoscopic approach. The mechanical behaviour of the woven reinforcement is analysed at the scale of the woven unit cell and introduced in finite elements that are composed of woven cells. The biaxial and the in-plane shear behaviour are analysed by specific experiments and by 3D finite element computations of the woven unit cell. Two simplified approaches are developed. In the first one, only the tension stiffness is considered and in the second one the in-plane shear is added. The example of a square box forming shows that the shear is important to describe the wrinkles that appear if the shear-locking angle is exceeded.

2. Simplified mechanical behaviour of woven reinforcements based on tensile surfaces

2.1. Simplified form of the dynamic equation

Glass, carbon and aramid fibres have very interesting mechanical performances. Consequently, they are used in components strongly loaded that have to be light. The diameter of these fibres is very small (5 to 7 μm for carbon fibres, 5–25 μm for glass fibres) in comparison with their length. Consequently, these fibres can only be loaded in tension in the direction of the fibre $\mathbf{h}_1$ (Fig. 1(a)). The Cauchy stress in the fibre has the following form:

$$\sigma = \sigma^{11}\mathbf{h}_1 \otimes \mathbf{h}_1, \quad \sigma^{11} \geqslant 0. \tag{1}$$

The fibres are put together to form yarns. Those can have different internal structures. Those used in case of composite reinforcements are often obtained by juxtaposition of a large number of fibres (thousands). This permits a relative sliding of fibres in case of yarn bending. Consequently, the stress in the yarn (Fig. 1(b)) remains in form (1). In the case of two yarn networks directed by $\mathbf{h}_1$ and $\mathbf{h}_2$ (Fig. 1(c)), the stress state can be assumed to have the following form:
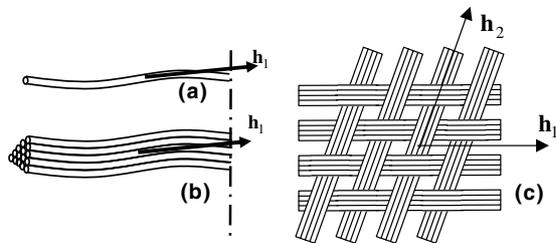

Fig. 1. (a) Single fibre, (b) yarn made of juxtaposed fibres, (c) woven yarns.

$$\sigma = \sigma^{11}\mathbf{h}_1 \otimes \mathbf{h}_1 + \sigma^{22}\mathbf{h}_2 \otimes \mathbf{h}_2. \tag{2}$$

Eq. (2) assumes that the in-plane shear influence is neglected (and especially the interactions between neighbouring yarns). This hypothesis will be questioned in Section 5. Based on Eq. (2) a simplified dynamic equation can be written for a part made of ncell elementary woven cells

$$\forall \, \eta/\eta = 0 \text{ on } \Gamma_u:$$

$$\sum_{p=1}^{\text{ncell}} {}^p\varepsilon_{11}(\eta)^p T^{11p}L_1 + {}^p\varepsilon_{22}(\eta)^p T^{22p}L_2 - T_{\text{ext}}(\eta)$$

$$= \int_\Omega \rho \, \overset{\circ\circ}{u} \, \eta \, \mathrm{d}V, \tag{3}$$

where the tensions are defined as

$$T^{11} = \int_{A_1} \sigma^{11} \, \mathrm{d}S, \quad T^{22} = \int_{A_2} \sigma^{22} \, \mathrm{d}S, \quad T^{11} \geqslant 0, \quad T^{22} \geqslant 0, \tag{4}$$

where A_1 and A_2 are the sections of the warp and weft yarns. $\mathbf{\eta}$ is the virtual displacement ($\eta = 0$ on the frontier with prescribed displacements). p is the number of the woven cell, L_1, L_2 are the length of the woven cell in warp and weft direction, ρ is the mass per volume unit, $\overset{\circ\circ}{u}$ is the acceleration and $\varepsilon_{\alpha\beta}$ ($\alpha,\beta = 1$ or 2) are the covariant strain components, i.e. $\varepsilon = \varepsilon_{\alpha\beta}\mathbf{h}^\alpha \otimes \mathbf{h}^\beta$ (with $\mathbf{h}_\alpha \cdot \mathbf{h}^\beta = \delta_\alpha^\beta$). $T_{\text{ext}}(\eta)$ is the virtual work of exterior loads.

2.2. Tension surfaces

Because of the weaving, the tensions T^{11} and T^{22} are related to axial strains in both warp and weft directions

$$T^{11}(\varepsilon_{11}, \varepsilon_{22}) \quad \text{and} \quad T^{22}(\varepsilon_{11}, \varepsilon_{22}). \tag{5}$$

Those two functions, that define the behaviour of the fibre fabric within the assumptions made in Section 2.1, give the two tensile surface of the fabric. There is a single surface if the fabric is balanced, i.e. if the warp and weft directions are identical. The goal of the two next sections is the determination of these surfaces.

3. Biaxial tensile tests

3.1. Multiscale non-linear phenomenon

When tensile tests are performed on a fabric in the yarn direction (Fig. 5) the load versus strain curves a strongly non-linear zone at the beginning of the loading followed by a linear behaviour. The non-linearity when loading is beginning can be explained by phenomena occurring at lower scales. Because of the weaving the fabric involves yarn undulations. Under tension, the yarn tends to become straight. In the limit case where the other direction is free to move, the tense yarns be-

come completely straight and the yarn in the other direction become very undulating (Fig. 2(b)). If both directions are tense (biaxial strains), a balance state is obtained. Both directions are subjected to undulation variations (usually undulation decreasing) (Fig. 2(a)). It is clear that the phenomenon is biaxial and that warp and weft yarns are in interaction. Occurring at the scale of the unit woven cell, these non-linear phenomena due to geometrical non-linearities are called mesoscopic. They are related and amplified by phenomena at fibre scale (microscopic scale). Because of tensile loads in the yarn direction and of compressive loads at contact between warp and weft yarns, the fibres are rearranged, the voids between fibres are reduced and the transverse shape of the yarn changes. These motions within a tow also show present in cable behaviour [6]. The non-linearities at this scale are due to contact-friction between fibres. They contribute to non-linearities at mesoscopic non-linearities. The set of these phenomena give the material non-linearity observed at the fabric macroscopic scale when it is stretched.

3.2. Experiments

Tensile tests are performed using a device able to stretch woven material in warp and weft directions at the same time in order to highlight characteristics listed in Section 2.1. The device (Fig. 3) is based on two hinged lozenges [7,8] that impose a biaxial strain state to a cross shape woven specimen. One direction has adjustable lengths in order to prescribe different strain ratios in warp and weft directions. Load sensors placed just behind the specimen give the total load in each direction. The strain measures are made using optical method [9] or mechanical extensometers [7]. Only the central part of the cross specimen is woven. The goal of the non-woven parts is to transmit the tensile loads while permitting the transverse deformation of the specimen. This cross shape specimen is well suitable for fabrics because of this

possibility and because the shear stiffness of fabric is very small as opposed to continuous materials such as metals. It is possible to modify the angle between warp and weft directions. Experiments have been performed for angles from 90° to 60° [7]. The influence of this angle on the biaxial tensile properties is weak for the tested materials and will be first neglected.

Fig. 3. Biaxial tensile device on cross shape specimens.
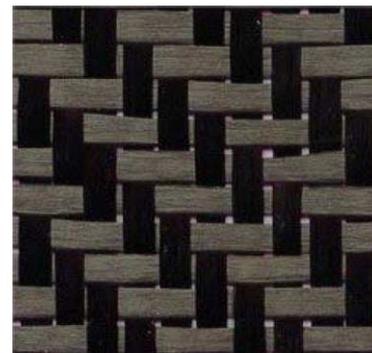
Density (yarn/mm): 0.35
Crimp (%): 0.35
Yarn strength: 420N
Yarn stiffness: 54000N
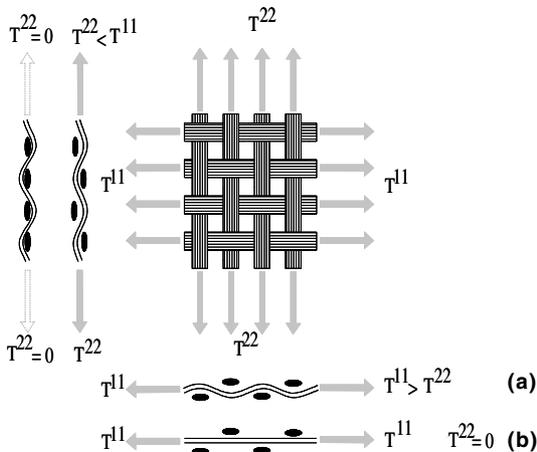
Fig. 4. 2×2 twill of carbon.

Fig. 2. Undulation variations in case of warp and weft tensions.
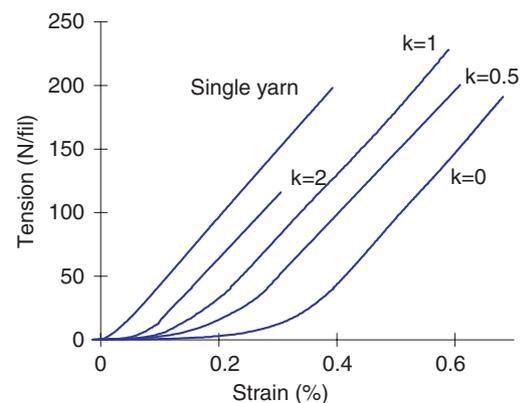

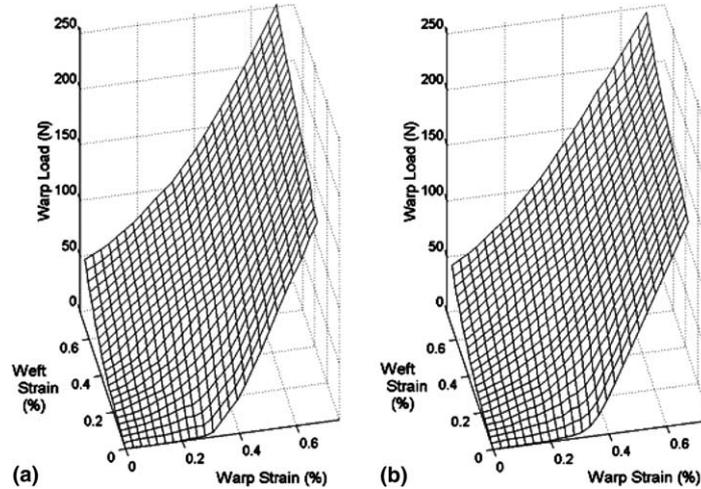Fig. 5. Tension versus strain for different ratio $k = \varepsilon_{11}/\varepsilon_{22}$.

Fig. 6. Tension surface $T(\varepsilon_{11}, \varepsilon_{22})$ for a 2×2 twill of carbon. (a) experiment, (b) 3D FE analysis.

Biaxial tensile tests results are given Fig. 5 in the case of a 2×2 twill of carbon. The yarn and the weaving are identical in warp and weft directions (Fig. 4) and the results will be only given in one direction. The yarn is composed of 6000 high strength carbon fibres combined without torsion. Although the yarn alone has a nearly linear tensile behaviour, the tension-strain curves obtained for the fabric are clearly non-linear at the beginning of the loading while the curves become linear for higher loads. This non-linearity is a consequence of non-linear phenomena occurring at lower scales (undulation variations, yarn crushing). The size of the non-linear zone is important compared with fracture strain (about 0.8%). It depends on the ratio k of the prescribed strains ($k = \varepsilon_{11}/\varepsilon_{22}$). This clearly shows the biaxial nature of the fabric tensile behaviour. Each direction influences the tensile behaviour of the other. The non-linear zone is maximal when one direction is stretched while the other is free. Actually the yarns in the tensile direction become straight. After the non-linear zone, the rigidity of the fabric is those of the only yarn. The strain reached at the transition is characteristic of the fabric crimp. The non-linear zone is less important as the k ratio increases.

From the tension-strain curves for different ratios k, it is possible to extrapolate the tension surfaces $T^{\alpha\alpha}(\varepsilon_{11}, \varepsilon_{22})$ [10]. The obtained surface for the 2×2 twill of carbon is shown Fig. 6(a). Other experimental results concerning different fabrics (balanced and un-balanced) can be found in [7].

4. 3D finite element analysis of the woven unit cell

3D finite element analysis of the woven unit cell is an alternate method to determinate tensile surfaces [11]. This approach allows to determine the tensile biaxial behaviour of a fabric prior to manufacturing. It also permits to better understand the behaviour of the fabric at mesoscopic scale.

The main difficulty of these computations consists in reproducing the fibrous nature of the yarns (lack or weakness of some stiffness) using 3D continuous finite elements. This specific behaviour is obtained for shear modulus nearly equal to zero and transverse Young modulus weak in comparison with the tensile Young modulus. The transverse law appears to be an important point for a good modelling of the unit woven shell. The following form permits to model the strong hardening of the fibrous yarn in transverse direction

$$E_i = E_0 \mid \varepsilon_{ii}^n \mid \varepsilon_{11}^m + E_\varepsilon, \tag{6}$$

where E_0, m and n are three material parameters. The direction of the yarn is denoted by index 1, i is a perpendicular direction ($i = 2$ or 3). E_ε is the initial transverse modulus (very weak). For a given yarn, the values of the orthotropic behaviour are identified using yarn tensile and crushing experiment and inverse approaches [12,11]. It is also very important to follow carefully the fibre directions during the deformation. The mechanical behaviour of the yarn is very sensitive to these directions. Two approaches have been developed. One uses reinforcements [11] and the other is based on the use of an objective derivative based on the fibre rotation [13]. Because some rigidities are nearly equal to zero, some numerical instabilities often appear. This is avoided by hourglass control (adding judicious artificial shear stiffness) [14]. Fig. 7 shows the analysis of the elementary 2×2 carbon twill unit cell under a biaxial tension with $k = 1$. The obtained tension surface (Fig. 6(b)) is in good agreement with those obtained from biaxial tensile experiments (Fig. 6(a)). Fig. 7 shows that the crushing of the yarn is important (45% maxi). In this case ($k = 1$), the behaviour non-linearity is due to this
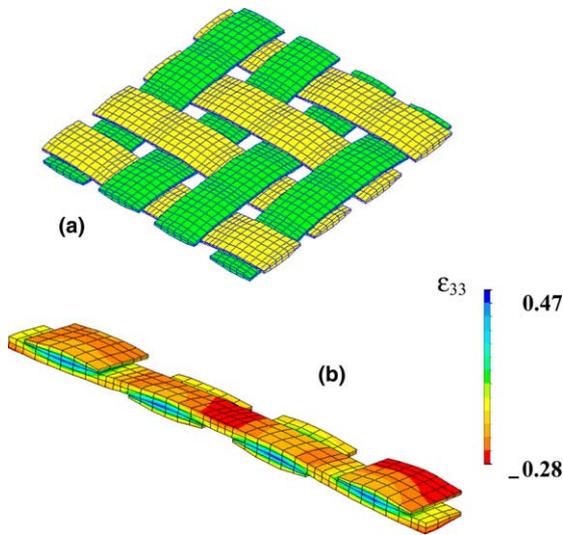
Fig. 7. 3D simulation of an equibiaxial tensile test on a 2×2 glass twill unit cell (a) finite element mesh (b) tranverse strain.

crushing. This transverse yarn section change is one of the main aspects of the mesoscopic behaviour of the fabric and it must be described carefully. Other 3D woven unit cell F.E. analysis can be found in [11,15]. This type of analysis is realised for knitted materials in [13,16].

5. In plane shear behaviour

5.1. In plain shear deformation of a fabric

The larger rigidities of a woven reinforcement are the tensile stiffness. They are those that guide the shape changes for instance during a composite forming. The shear stiffness of the fabric is weak at least in the unde-

formed state. Consequently, large in- plane strains occur and are the main forming mode of fabrics. If the shear rigidity is weak, it can be studied as a complement to tension rigidity. In addition the in-plane shear stiffness can be increased if the fabric is coated with resin (non-polymerized prepreg or thermoplastic over fusion temperature) or really increased if the shear strain exceed the shear limit angle (or locking angle). In this case, we shall see that it is very important to take the shear rigidity into account. Studies concerning in-plane shear behaviour of woven reinforcements are numerous, probably because it is the main deformation mode of fabrics [17–20]. In this section the experiment in-plane shear behaviour of dry woven reinforcements is analysed both at macroscopic level and yarns scales (micro and macroscopic scale). An internal virtual shear work is then added to the dynamic equation.

5.2. Picture frame experimental analysis

The shear test experimental device used in this study is called picture frame (Fig. 8). It is based on the principle of a deformable frame with four identical hinged sides. The yarns of the fabric specimen are parallel to the sides. Several studies tend to show that this system is the most satisfactory in order to prescribe a homogeneous shear to a woven reinforcement [21]. The picture frame is set on a classical tensile machine. A tension is applied to the yarns before the shear test. The surface of the specimens is 0.2×0.2 m^2.

5.3. Optical strain measurements

An optical system records pictures at two scales (Fig. 8). These pictures concern the whole specimen (macro scale) or only few woven cells (12.4×9.5 mm^2)
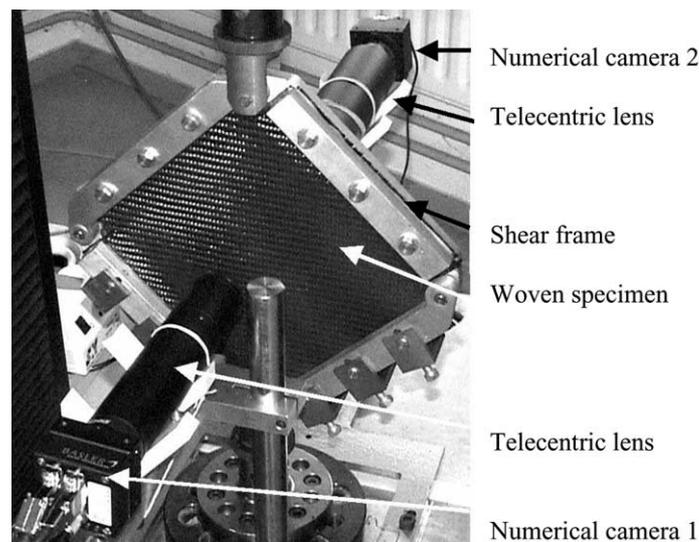

Fig. 8. Shear frame device equipped with an optical system.

(meso scale). The measure domain can be restricted to a single yarn (micro scale). Two pictures (macro and micro) are taken at the same time using cameras on both sides of the specimen (Fig. 8). These pictures are used to compute the displacement and strain fields using an image correlation method [22]. The macroscopic measures give the shear value versus load on the picture frame. These measures concern the shear field and it is possible to check the homogeneity of the shear in the specimen. This has permitted to modify the picture frame technology (especially the specimen fixing system) in order to achieve a correct homogeneity of the shear [23,24].

5.4. Micro-macro analysis

Fig. 9 gives the load versus shear strain curve in the case of a glass plain weave (density of the yarns $n = 0.25$, crimp $s = 0.5\%$, surface density: $w = 600$ g/m^2, linear density $w = 1200$ tex). The curve can be divided in three zones. Fig. 10 shows the displacement field within the yarn (micro scale) during stage 1 (beginning of the loading). In this purpose, the mean value of the displacement in the yarn is subtracted to the measured displace-
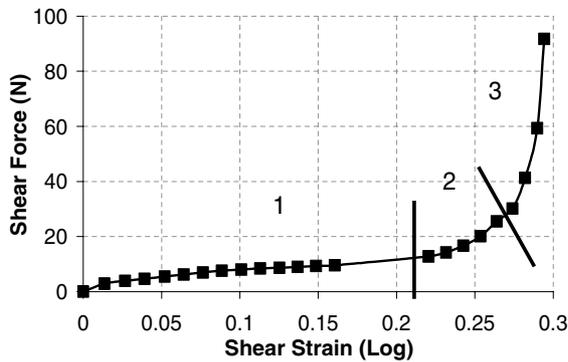
ments. One can see that the yarns are submitted to a rigid body rotation that globally gives an in-plane shear on the fabric specimen. There is no shear within the yarns. Consequently, the corresponding loads on the frame remain weak because the only resistance to shear is due to friction between warp and weft yarns. The beginning of zone 2 corresponds to the shear limit angle or shear-locking angle. The yarns start to be in contact with their neighbouring and are laterally compressed (Fig. 11), partially first (zone 2) then totally (zone 3). This explains the very fast shear load increasing and consequently the shear stiffness. In practice wrinkles appear in zone 3 due to shear locking.

5.5. Taking into account the shear in the dynamic equation

The simplified form of the dynamic equation (3) only takes into account the tension interior load virtual work in each woven cell. The following form (6) takes the in plane shear into account

$$\sum_{p=1}^{\text{ncell}} {}^p\varepsilon_{11}(\eta)^p T^{11p} L_1 + {}^p\varepsilon_{22}(\eta)^p T^{22p} L_2 + \sum_{p=1}^{\text{ncell}} {}^p\gamma(\eta)^p C - T_{\text{ext}}(\eta)$$

$$= \int_\Omega \rho \, \overset{\circ\circ}{u} \, \eta \, \mathrm{d}V, \tag{7}$$

where ${}^p C$ is the couple due to the shear for the woven cell p and ${}^p\gamma(\eta)$ is the rotation between warp and weft yarns in the virtual displacement field η. The load versus shear strain (Fig. 9) permits to link the couple to the warp-weft rotation [25]. Both simplified forms of the dynamic equation (3), taking into account only the tensile virtual interior load and (6) both tensile and shear, permit to construct simplified finite elements that are specific to woven materials and that can be used in an explicit dynamic approach [15,25]. The following deep drawing example show the obtained results with and without taking the shear into account.
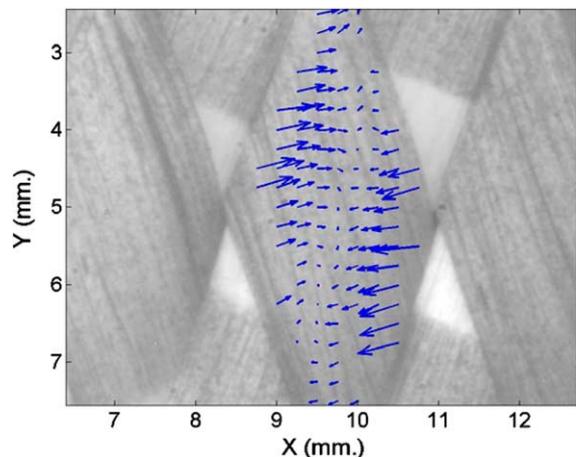

Fig. 9. Shear behaviour law of a glass plain weave.
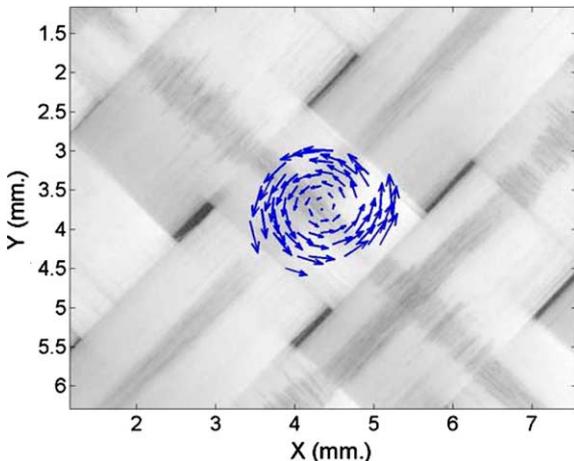
Fig. 10. Displacement field in a yarn during part 1.

Fig. 11. Displacement field at micro-scale after the locking angle.

5.6. Deep drawing of a square box

The test showed Fig. 12 is a classical benchmark for sheet metal forming. It has been proposed at Numisheet 93 conference [26]. Accounting for the strongly non-developable geometry, this test is very severe especially for fabric forming because it asks very large angle variations between warp and weft yarns in the radius of the square box. If those radiuses are reduced, the shear strains that are necessary to shape the part are quickly larger than the limit angle of the fabric. The forming of a plain weave fabric (the characteristics of which are given in Section 5.4). is simulated with both the approach based on tensile energy only and the approach taking both shear and tensile energy into account. Fig. 13 presents in both cases the computed deformed shape after forming. Because of the geometry (strongly double curved) the locking angle of the plain weave fabric is exceeded. This leads to rather different results for
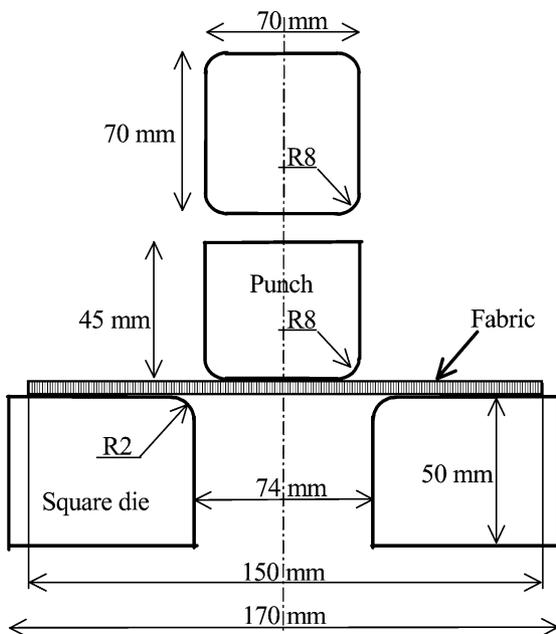

Fig. 14. Angle between warp and weft yarns. Formulation in tension (at the top) and in tension + shear (at the bottom).

Fig. 12. Square box deep drawing. Geometry of the tools.
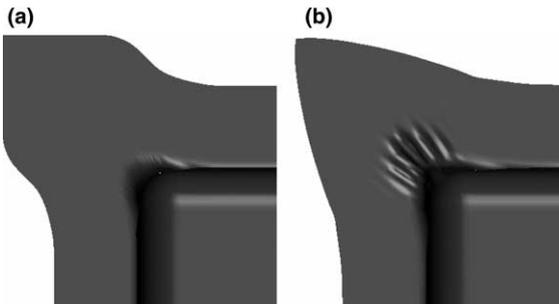
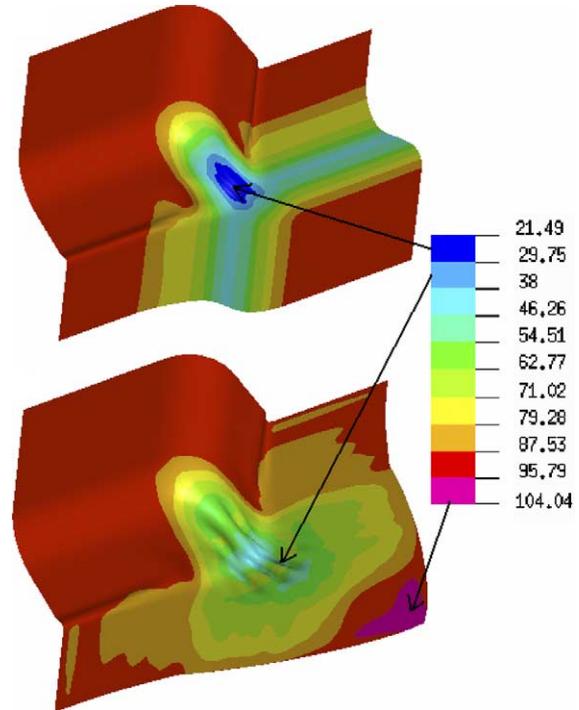Fig. 13. Final shape of the fabric. Formulation in tension (a) and in tension + shear (b).

both approaches. There is no wrinkle when using the approach based on the only tension because there is no source of instability. On the contrary the computed solution obtained when taking shear into account comprises some wrinkles. These are due to shear locking that leads to out-of plane solutions in order to reduce this shear. Fig. 14 shows that the rotation angles are clearly reduced when the shear stiffness is taken into account. In the present case, the second approach is better in order to stick to reality. The reason for this is that the simulation concerns a forming process for which it is necessary to exceed the shear limit angle. That is generally not the case for a successful part. It can also be noticed that the tension only approach also detects the limit angle exceeding. The contribution of the shear term mainly shows in the description of the deformed shape after the wrinkle appear.

6. Conclusions

The mechanical behaviour of fabrics in tension and in shear is much affected by phenomena occurring at meso (and micro) scale, especially the contact friction and crushing of the yarns due to weaving and deformation. In tension, the behaviour is non-linear because of the undulation changes. This non-linearity depends on the biaxial strain ratio. The surfaces that quantify this tensile behaviour have been obtained by biaxial tensile tests

and 3D finite element computations of the unit woven cell. Non-linearities at mesoscopic level influence the shear behaviour as well. The shear stiffness is weak for moderate angles. Optical measures have shown that, in this stage, the yarns are submitted to a rigid body rotation. When the shear angle increases, the yarns come into contact with their neighbouring. They are compacted and the shear stiffness is strongly increased. Forming simulations can be based on the simplified formulations based on these two deformation modes. Specific finite elements have been developed by a mesoscopic approach, i.e. by considering each woven cell in tension (and possibly in shear). It is necessary to take the in-plane shear into account if the shear angle exceed the locking angle. It is now necessary to precisely identify the cases for which taking only the tensile stiffness into account is necessary and those for which the shear stiffness has to be taken into account. In this case the assumption that has been made here and that consists in neglecting the bending stiffness would have to be verified, especially in relation to the wrinkle shape.

Acknowledgement

References

[1] Gauvin R, Trochu F, Lemenn Y, Diallo L. Permeability measurement and flow simulation through fibre reinforcement. Polym Compos 1996;17:34–42.

[2] Bickerton S, Simacek P, Guglielmi SE, Advani SG. Investigation of draping and its effects on the mold filling process during manufacturing of a compound curved composite part. Composites A 1997;28A:801–16.

[3] Bergsma OK, Huisman J. Deep drawing of fabric reinforced thermoplastics, Brebbia CA et al. (editors). In: Proceedings of the 2nd international conference on computer aided design in composite material technology, Springer, 1988; p. 323–33.

[4] Van Der Ween F. Algorithms for draping fabrics on doubly curved surfaces. Int J Numer Meth Eng 1991;31:1414–26.

[5] Borouchaki H, Cherouat A. Une nouvelle approche pour le drappage des structures composites. Revue des composites et matériaux avancés, Hermès 2002;32:407–22.

[6] Durville D. Modélisation du comportement mécanique des câbles métalliques, Actes du 3ième colloque national en calcul des structures, Giens 1997;1:139–44.

[7] Buet K, Boisse Ph. Experimental analysis and models for biaxial mechanical behaviour of composite woven reinforcements. Exp Mech 2001;41(3):260–9.

[8] Ferron G. Dispositif de traction biaxiale DAX2, Document Techmetal, Mézières-Lès-Metz; 1992.

[9] Launay J, Lahmar F, Boisse P, Vacher P. Strain measurement in tests on fibre fabric by image correlation method. Adv Compos Lett 2002;11(1):7–12.

[10] Hivet G. Modélisation et simulation du comportement mécanique des renforts tissés, Thèse de l'Université d'Orléans; 2002.

[11] Gasser A, Boisse P, Hanklar S. Mechanical behaviour of dry fabric reinforcements. 3D simulations versus biaxial tests. Comput Mater Sci 2000;17(1):7–20.

[12] Schnur DS, Zabaras N. An inverse method for determining elastic material properties and a material interface. Int J Numer Meth Eng 1992;33:2039–57.

[13] Hagege B. Simulation du comportement mécanique des milieux fibreux en grandes transformations: application aux renforts tricotés. Ph.D. thesis of Ecole Nationale Supérieure d'Arts et Métiers; 2004.

[14] Flanagan DP, Belytschko T. A uniform strain hexahedron and quadrilateral with orthogonal hourglass control. Int J Numer Meth Eng 1981;17:679–706.

[15] Boisse P, Gasser A, Hivet G. Analyses of fabric behaviour: determination of the biaxial tension-strain surfaces and their use in forming simulations. Composites A 2001;32(10):1395–414.

[16] Hagege B, Boisse P, Billoët JL. Specific simulation tools for the shaping process of knitted reinforcements. In: Proceedings of the 6th international ESAFORM conference on material forming, Salerno; 2003.

[17] McBride TM, Chen J. Unit-cell geometry in plain-weave fabrics during shear deformations. Compos Sci Technol 1997;57(3):345–51.

[18] Prodromou AG, Chen J. On the relationship between shear angle and wrinkling of textile composite preforms. Composites A 1997;28(5):491–503.

[19] McGuinness GB, Bradaigh CMO. Development of rheological models for forming flows and picture-frame shear testing of fabric reinforced thermoplastic sheets. J Non-Newton Fluid Mech 1997;73(1–2):1–28.

[20] McGuinness GB, Bradaigh CMO. Characterisation of thermoplastic composite melts in rhombus-shear: the picture-frame experiment. Composites A 1998;29(1–2):115–32.

[21] Long AC. Characterisation and modelling of fabric deformation during forming of textile composites. Int J Forming Process 2002;4:285–301.

[22] Vacher P, Dumoulin S, Arrieux R. Determination of the forming limit diagram from local measurement using digital image analysis. Int J Forming Process 1999;2(3–4):395–408.

[23] Dumont F. Expérimentations et modèles de comportement de renforts de composites tissés, Thèse de doctorat, Université de Paris VI, France; 2003.

[24] Lussier DS, Chen J. Material characterization of woven fabrics for thermoforming of composites. J Thermoplast Compos Mater 2002;15:497–509.

[25] Zouari B, Dumont F, Daniel JL, Boisse P. Studies of woven fabric shearing by optical method and implementation in a finite element program. Proceedings of Esaform 2003;6:875–8.

[26] Numisheet'93, Numerical simulation of 3-D sheet metal forming processes – verification of simulation with experiments, Makinouchi A, Nakamachi E, Onate E, Wagoner RH (editors), Japan; 1993.